Use of Resonant Terms in a 2DOF Control Scheme for the Current Control of an Active Power Filter

1st Fco. Javier López-Alcolea
*Institute of Energy Research and
Industrial Applications. UCLM*
Ciudad Real, Spain
FJavier.Lopez@uclm.es

2nd Emilio J. Molina-Martínez
*Institute of Energy Research and
Industrial Applications. UCLM*
Ciudad Real, Spain
EmilioJose.Molina@uclm.es

3rd Javier Vázquez
*Institute of Energy Research and
Industrial Applications. UCLM*
Ciudad Real, Spain
Javier.Vazquez@uclm.es

4th Pedro Roncero-Sánchez
*Institute of Energy Research and
Industrial Applications. UCLM*
Ciudad Real, Spain
Pedro.Roncero@uclm.es

5th Alfonso Parreño Torres
*School of Industrial Engineering
University of Castilla-La Mancha*
Albacete, Spain
Alfonso.Parreno@uclm.es

6th Ismael Payo
*Institute of Industrial and
Aerospace Engineering, UCLM*
Toledo, Spain
Ismael.Payo@uclm.es

Abstract—This paper proposes a control scheme for the current injected by an Active Power Filter (APF) that has an LCL filter at its output. The proposed structure relies in a Two-Degrees-of-Freedom (2DOF) controller in which resonant terms are included. The 2DOF scheme follows the current reference at the fundamental frequency of the grid and damps the resonance phenomenon of the LCL filter, whereas the resonant regulators allow a proper tracking of the harmonics. This is achieved with only the measurement of the current injected by the APF into the grid, without the need for additional measurements or observers. In order to assess the performance of the controllers, a Hardware-In-the-Loop (HIL) emulation has been carried out. The results show a good time response, allowing the compensation of current disturbances at both the fundamental frequency and its harmonics.

Index Terms—Active Power Filter, Current Control, Two-Degrees-of-Freedom, Resonant Regulators

I. INTRODUCTION

The use of shunt Active Power Filters (APF) for compensating the current disturbances caused by the different devices connected to the grid has received a notorious attention from the researchers. They would be placed in an industrial or household environment and its aim is to supply the current demanded by the loads that corresponds to the negative and zero sequence components, as well as current harmonics and reactive power. In this manner, from the source point of view, the loads will demand only the current that corresponds to the active power of the positive sequence component at the grid frequency. Consequently, the perturbations caused by the loads will be confined in the environment in which they are placed, avoiding its propagation throughout the distribution grid.

The operation of a shunt APF can be split into three well-differentiated parts [1]. The first one consists on calculating the current that must be injected into the grid for compensating

the current disturbances. This reference current feeds a control scheme that compares it with the current flowing through each phase of the APF and generates a control signal. Then, the control signal is an input to a third stage, that generates the firing signal of the switches of the APF.

Different control strategies for the current injected by the APF can be found in the literature. For example, in [2] the use of Proportional-Integral (PI) regulators in a synchronous reference frame is proposed for achieving a zero-error tracking of the current component at the grid frequency and Proportional-Resonant regulators for canceling the current harmonics. Other techniques such as the predictive [3] or repetitive [4] control schemes have also been proposed. By choosing an appropriate topology, the control of the APF can be addressed independently in each phase. Thus, the reference frame transformations can be avoided. Moreover, if a high-order filter (e.g, an LCL topology) is placed between the APF and the grid, the damping of the filter should be addressed [3]. Hence, active or passive damping methods must be implemented.

This paper aims to propose a control strategy for an APF that is connected to the utility grid through an LCL filter. This is achieved by using a Two-Degrees-of-Freedom (2DOF) control scheme that tracks the fundamental frequency component of the reference current and damps the resonance phenomenon of the LCL filter by only measuring the current at its output. The tracking of the harmonic components is achieved by adding resonant regulators to the proposed control structure. The 2DOF controller provides a fast response for the tracking of the fundamental frequency, which enhances the time response of the APF when compared to the use of resonant regulators. Moreover, this control scheme can be applied independently to each phase of the APF. Therefore, the issues of coupling equations when a synchronous reference frame is used are not present, and would be used also in single-phase systems.

The remainder of this paper is structured as follows: Section II describes the proposed system to which the control strategy will be applied. In section III, the design procedure of the control scheme is addressed, whereas in Section IV a design example is given. The results obtained after emulating the proposed system in a Hardware-In-the-Loop (HIL) platform are shown in Section V, whereas the conclusions extracted from this work are addressed in Section VI.

II. SYSTEM DESCRIPTION

The system considered in this paper corresponds to a three-phase four-wire system connected to an utility grid with a grid frequency f_0. The operation of the loads will cause a series of current disturbances (negative and zero sequence components, reactive power, and harmonics) that must be compensated by the APF.

The topology selected for the APF corresponds to a four-leg split-capacitor (4LSC) structure with an LCL filter placed at its output (see Fig. 1). The 4LSC topology has a significant advantage when compared to other topologies: if the voltage of capacitors C_1 and C_2 is balanced (that is, $V_{C1} = V_{C2}$), each phase of the inverter can be controlled independently [5]. Thus, the simple and widely extended Sinusoidal Pulse Width Modulation (SPWM) can be used [6]. Moreover, the independent control of each phase allows to design the current controller for the phases A, B and C as if they were independent single-phase systems. This characteristic is also present in the Three-Leg Split Capacitor (3LSC) topology, in which the fourth leg is omitted [7]. However, it does not allow the active control of the neutral current in the inverter. Thus, this characteristic is lost in the 3LSC topology when a significant current flows through the neutral wire owing to a current imbalance in the inverter phase currents.

A. System Modeling

The generation of the reference current for the APF has been addressed in [8]. It extracts the current that corresponds to the active power of the positive sequence component at the fundamental frequency of the grid and substracts it from the total current demanded by the loads. As a result, the reference current for the APF is obtained. The aim of this paper is to describe the operation of the control stage and how it can be used to compensate harmonics, reactive power and positive, negative and zero sequence components. Providing that $V_{C1} = V_{C2}$, the control of the current in each phase of the APF can be addressed independently. Thus, the control scheme for the
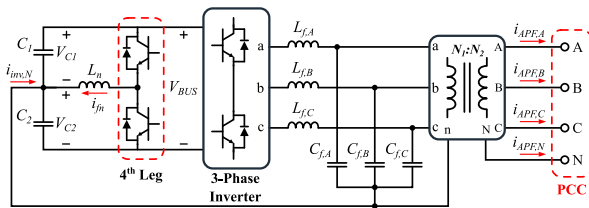
current injected in the phases A, B and C of the APF are decoupled single-phase systems.

The objective is to control the current at the output of the phase x of the APF, $i_{apf,x}(t)$, where x is A, B or C. This is achieved through applying a voltage $v_{inv,x}(t)$ at the output of the corresponding leg of the APF. The control scheme will measure $i_{apf,x}(t)$ and generate a control signal that will serve as the reference voltage for the SPWM modulation.

The LCL filter placed in each phase is composed of an inverter-side inductance, L_f, a capacitor, C_f and a single-phase transformer with a winding ratio $r = N_2/N_1$ and leakage inductances L_{d1} and L_{d2}. The Equivalent Series Resistances (ESRs) of L_f, C_f, L_{d1} and L_{d2} are R_{Lf1}, R_{Cf}, R_{Ld1} and R_{Ld2}, respectively.

The transformers are modeled by neglecting the effect of their magnetizing inductances. Thus, by reflecting the secondary coil on the primary, the scheme shown in Fig. 2 can be obtained.

As a result, the grid-side total inductance L_T and its ESR R_{LT} can be expressed as follows:

$$L_T = L_{d1} + L'_{d2} = L_{d1} + \frac{L_{d2}}{r^2} \tag{1}$$

$$R_{LT} = L_{d2} + R'_{Ld2} = L_{d2} + \frac{R_{Ld2}}{r^2} \tag{2}$$

The transfer function from the output voltage of the inverter $V_{inv,x}(s)$ to the current at the output of the APF $I_{apf,x}(s)$ can be expressed in the continuous-time domain as [9]:

$$P(s) = \frac{I_{apf,x}(s)}{V_{inv,x}(s)} = \frac{B_1 s + B_0}{s^3 + A_2 s^2 + A_1 s + A_0} \tag{3}$$

where:

$$B_1 = \frac{R_{Cf}}{L_f L_T}; \; B_0 = \frac{1}{L_f L_T C_f}; \; A_0 = \frac{R_{Lf} + R_{LT}}{L_f L_T C_f}$$

$$A_1 = \frac{1}{L_f C_f} + \frac{1}{L_T C_f} + \frac{R_f R_T + R_{Cf}(R_{Lf} + R_{LT})}{L_f L_T} \tag{4}$$

$$A_2 = \frac{R_{Cf} R_{Lf}}{L_f} + \frac{R_{Cf} R_{LT}}{L_T}$$

After discretizing the plant $P(s)$ and taking one sample time, T_s, as the delay caused by the PWM modulation and the calculation of the control signal, the discrete-time transfer function $P(z)$ can be obtained:

$$P(z) = \frac{I_{apf,x}(z)}{V_{inv,x}(z)} = z^{-1} \frac{b_2 z^2 + b_1 z + b_0}{z^3 + a_2 z^2 + a_1 z + a_0} \tag{5}$$

Fig. 1. Topology selected for the APF.
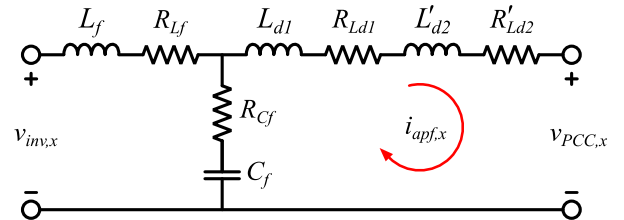
Fig. 2. Simplified scheme of the LCL filter.

III. DESIGN OF THE CONTROL STAGE

The block diagram of the proposed control stage is depicted in Fig. 3. It is composed of a 2DOF controller and a series of resonant regulators labeled as $R_h(z)$, where $h > 1$ is the index of the corresponding harmonic of f_0.

A. 2DOF controller

The objective of the 2DOF controller is to track a current reference whose fundamental frequency is f_0. The 2DOF scheme allows to choose the location of the poles of the equivalent closed-loop system, $H(z)$, in order to obtain a fast time response (less than 20 ms). It is composed of two regulators, one located in the direct path, $R_d(z)$, and a second whose input is the feedback signal of the measured current, $R_f(z)$. The controller located in the direct path has been defined as $R_d(z) = R_\omega(z) \cdot R_p(z)$ in order to separate the resonant term $R_\omega(z)$, whose parameters are known, from $R_p(z)$. The controllers are defined as follows:

$$R_\omega(z) = \frac{R_{\omega,n}(z)}{R_{\omega,d}(z)} = \frac{z - 1}{z^2 + z c_0 + 1} \tag{6}$$

$$R_p(z) = \frac{R_{p,n}(z)}{R_{p,d}(z)} = \frac{z K_1 + K_0}{z^3 + z^2 \rho_2 + z \rho_1 + \rho_0} \tag{7}$$

$$R_f(z) = \frac{R_{2,n}(z)}{R_{2,d}(z)} = \frac{z^3 K_5 + z^2 K_4 + z K_3 + K_2}{z^3 + z^2 \rho_2 + z \rho_1 + \rho_0} \tag{8}$$

where $c_0 = -2\cos(2\pi f_0 T_s)$ and the coefficients of the transfer functions of $R_p(z)$ and $R_f(z)$ are obtained by selecting the location of the poles of $H(z)$ and following the steps outlined in [9], [10]. The numerator and denominator of the equivalent closed-loop transfer function $H(z) = N(z)/F(z)$ are:

$$N(z) = P_n(z) R_{\omega,n}(z) R_{p,n}(z)$$

$$F(z) = P_d(z) R_{\omega,d}(z) R_{2,d}(z) + \tag{9}$$

$$+ P_n(z) \left[R_{p,n}(z) R_{\omega,n}(z) + R_{2,n}(z) R_{\omega,d}(z) \right].$$

The zero at $z = 1$ in the numerator of $R_\omega(z)$ will cause $H(z)$ to reject the DC component, whereas the resonant term $R_\omega(z)$ will cause the magnitude and phase to be 0 dB and 0° at
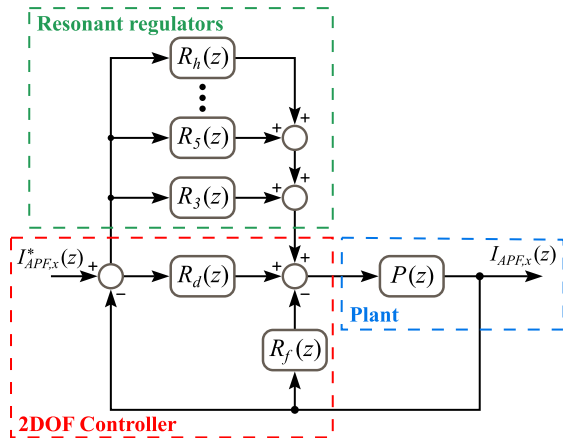
f_0. Hence, a pass-band behavior can be obtained by properly selecting the poles of $H(z)$.

B. Resonant terms

The use of the resonant terms, $R_h(z)$, is included in the control scheme in order to give the system the capability of tracking a reference current composed of a fundamental frequency f_0 and its harmonics. They are placed in parallel with $R_d(z)$ and its transfer function is defined as follows:

$$R_h(z) = \underbrace{\frac{1}{z^2 + c_h z + 1}}_{R_{\omega,h}(z)} \cdot \underbrace{k_h \frac{z - \beta_h}{z - \alpha_h}}_{R_{d,h}(z)} \tag{10}$$

It is composed of a resonant term $R_{\omega,h}(z)$ and a phase-lead compensation term $R_{d,h}(z)$. The resonant term is tuned at the frequency of the h-th harmonic of f_0 through the parameter $c_h = -2\cos(2\pi h f_0 T_s)$, whereas the parameters k_h, β_h and α_h are used to tune the term $R_{d,h}(z)$. Since f_0 and T_s are known, the coefficient c_h can be directly calculated. Thus, it is only necessary to define k_h, β_h and α_h. A possible solution can be $\alpha_h = 0$, which implies placing the pole of $R_d(z)$ as far as possible from the unit circle boundary. Therefore, it is only necessary to adjust k_h and β_h in each resonant term.

The design of R_h is addressed by adjusting the frequency response of the equivalent closed-loop system formed by $R_h(z)$ and $H_f(z)$, where $H_f(z)$ is the closed-loop transfer function of the internal control loop that comprises $R_f(z)$ and $P(z)$. According to [11], a band-pass behavior is desired for each resonant regulator in order to reduce the interaction between the controllers. However, the more selective the filter is, the slower its time response will be. Thus, it is needed to find a trade-off between the mutual influence among the different regulators, including the 2DOF control scheme, and how fast the controller tracks the corresponding harmonic component.

IV. DESIGN EXAMPLE

The APF is connected to the utility grid through an LCL filter whose design follows the steps outlined in [12], adapting the methodology from a wye to a star capacitor connection. The resulting parameters are shown in Table I. It is desired to follow the fundamental frequency and the third, fifth, seventh and ninth harmonics. The first step consists of choosing the location of the nine poles of the closed-loop equivalent system $H(z)$ to obtain the parameters of $R_d(z)$ and $R_f(z)$.

It is desired to reduce the interaction between the 2DOF controller and the resonant regulators. This is achieved by

Fig. 3. Proposed control scheme.

TABLE I
PARAMETERS OF THE LCL FILTER

Parameter	Value	Parameter	Value
Lf (mH)	2.6	R_{Lf} (mΩ)	80
C_f (μF)	46	R_{Cf} (mΩ)	50
L_{d1} (mH)	0.155	R_{Ld1} (mΩ)	200
L_{d2} (mH)	0.274	R_{Ld2} (mΩ)	300
r	$\sqrt{3}$	T_s (μs)	100

selecting $H(z)$ to have a pass-band behavior with a -3 dB cutoff frequency at 55 Hz. Thus, two poles are selected at $z = 0.966$. As $P(z)$ has a zero in $z = -0.2826$, another pole is chosen to be in the same location in order to achieve a zero-pole cancellation. Two other poles have been selected to be in 0.483 whereas the location for the four remaining poles are $z = 0$, which is the farthest location from the unit circle boundary. After following the steps outlined in [9], the parameters for $R_d(z)$ and $R_f(z)$ are shown in Table II.

The second step consists of tuning the parameters β_h and k_h for each resonant regulator $R_h(z)$. This part of the design will be carried out through establishing a series of restrictions to the frequency response of the equivalent system composed of $R_h(z)$ and $H_f(z)$:

- For the frequencies in the range $[0, (h-1)f_0]$ Hz, the gain must be lower than -15 dB.
- The gain is less than 1 dB in the range $((h-1)f_0, (h+1)f_0)$.
- For the frequencies above $(h+1)f_0$, the magnitude of the frequency response must be below -10 dB.

The first and the third restrictions aim to reduce the mutual interaction between regulators, whereas the second has the objective of limiting the undesired amplification of frequencies near the harmonics of f_0. Bearing in mind these restrictions, it is possible to adjust the parameters for each resonant controller following an iterative process:

1) The location of zero in the phase-lead term is selected through β_h.
2) The gain k_h is adjusted so that the magnitude of the frequency response meets the three restrictions. Fig. 4 shows the frequency response obtained after tuning the parameters β_3 and k_3 for the third harmonic.
3) If the time response of the system composed of $R_h(z)$ and $H_f(z)$ is considered slow, return to step 1.

A set of parameters that match all the restrictions is shown in Table III. The frequency responses of both $H(z)$ and the transfer function of the equivalent closed-loop system that includes the resonant terms, $H_{Tot}(z)$, are shown in Figs. 5 and 6. The addition of the terms $R_h(z)$ has little influence on the frequency response around and below 50 Hz. However, the magnitude and phase of $H_{Tot}(z)$ are now 0 dB and $0°$ at the frequencies of the chosen harmonics. Therefore, a proper tracking of a reference current with these components is ensured after introducing the resonant regulators. Moreover, the damping of the LCL filter is achieved with the 2DOF scheme without the need for additional measurements or observers.

TABLE II
PARAMETERS OF THE 2DOF CONTROLLER

Parameter	Value	Parameter	Value
c_0	-1.9990	ρ_0	0.1597
ρ_1	0.9207	ρ_2	1.4122
K_0	-3.2085	K_1	3.9929
K_2	-3.2085	K_3	31.4209
K_4	-19.8707	K_5	4.1270

TABLE III
PARAMETERS OF THE RESONANT REGULATORS

Harmonic	c_h	k_h	β_h
3	-1.9911	0.280	0.800
5	-1.9754	0.260	0.850
7	-1.9518	0.255	0.930
9	-1.9206	0.230	0.975
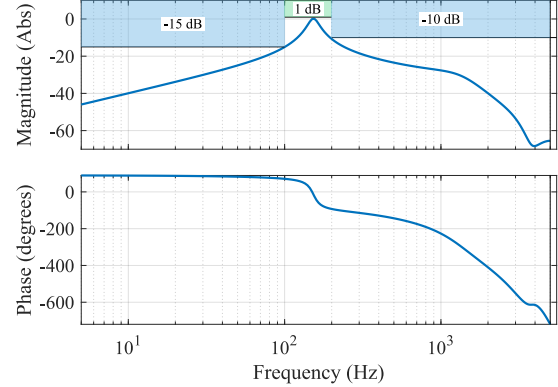
Fig. 4. Frequency response of the closed-loop equivalent system formed by $H_f(z)$ and $R_3(z)$.
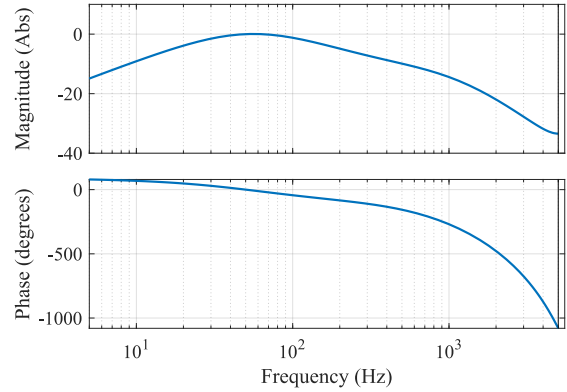
Fig. 5. Frequency response of $H(z)$.

Fig. 7 shows the time response for a reference current that contains only the 50 Hz component, while in Fig. 8 all the selected harmonics have been added with an amplitude of 0.15 A. As can be seen, the 50 Hz component is tracked in less than a period (20 ms), whereas the rest of the components are tracked within the first three periods (60 ms). This is because the 2DOF controller has been selected to have a faster time response than the resonant terms.

V. SIMULATION RESULTS

With the aim of validating the proposed control scheme, a Hardware-In-the-Loop (HIL) simulation has been carried out. The power system has been modeled in the Typhoon HIL 402 platform, whereas the controllers have been implemented in the dSPACE MicroLabBox. Three loads will be connected, causing a number of power quality issues:

- Load A is a three-phase device that demands a current that has positive, negative and zero sequence components
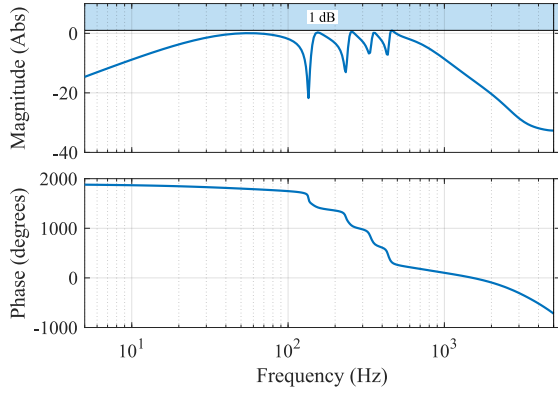
Fig. 6. Frequency response of $H_{Tot}(z)$.
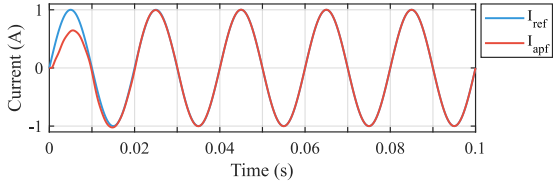
Fig. 7. Time response of the proposed control scheme for a 50 Hz reference current.
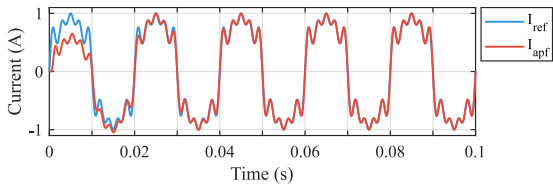
Fig. 8. Time response of the proposed control scheme for a 50 Hz reference current with a thirth, a fifth, a seventh and a ninth harmonic.

TABLE IV
HARMONIC CONTENT OF LOAD C

Harmonic	Amplitude (A)	$\hat{I}_h / \hat{I}_1$ (%)
1	20	–
3	4.32	21.6
5	2.14	10.7
7	1.44	7.2
9	0.76	3.8

whose RMS values are 5 A, 4 A and 2 A per phase, respectively.

- Load B is a three-phase balanced RL load with $R = 62\ \Omega$ and $L = 20$ mH.
- Load C is a three-phase balanced load whose harmonic content is shown in Table IV, where $\hat{I}_h$ is the amplitude of the harmonic h. The amplitude of the harmonics has been selected to match the maximum allowable values established by the standard IEC-61000-3-12 for a three-phase unbalanced load.

The line-to-line grid voltage has been set to 400 V and the grid frequency is 50 Hz. It will exhibit an ideal grid in order to see the response of the APF against the distorsion caused by the loads. Nonetheless, it would be interesting to check the response against distorted voltage waveforms in future works.

Since the control of the DC bus voltage is out of the scope of this paper, the DC bus of the APF is connected to an ideal DC source with a rated voltage of 550 V. Moreover, in the fourth leg of the inverter a control loop is applied that ensures $V_{C1} = V_{C2}$. Hence, it is guaranteed that each leg of the inverter can be controlled independently.

The three loads are connected when the operation of the APF begins at $t = 0$. The algorithm that generates the reference current initiates its operation well before the APF

starts injecting current. Therefore, its total delay does not affect the time response of the controllers. Fig. 9 shows the waveforms obtained for the source, load and APF currents during the first 100 ms. Since the APF DC side is fed with a voltage source, the current at its output corresponds only to the disturbances caused by the three loads. As can be seen, the waveform of the source current has been significantly improved after a period because the fast time response of the 2DOF controller makes the APF to follow the 50 Hz component quickly. Moreover, the current imbalance caused by the loads at the fundamental frequency has been also compensated.

The harmonic content of the three currents has been evaluated through the application of an FFT to the source, loads and APF currents with a measurement window of 200 ms. The obtained results, once the system has achieved the steady state, are shown in Fig. 10. The THD for the current demanded by the loads is 16.18 % for phase A and 20.26 % for phases B and C, while in the source is near 0.07 % due to the current harmonics compensation of the APF. As expected, the harmonic content of demanded by the loads matches those of the current injected by the APF. Thus, the only frequency component present in the current source is 50 Hz. This proves the correct tracking of all the harmonic components by both the 2DOF controller and the resonant regulators.

VI. CONCLUSIONS

In this paper, the current control of an APF that has an LCL filter placed at its output has been considered. The current controller must follow a reference current that contains the fundamental frequency and its harmonics, while damping the LCL filter. This has been addressed through the use of a 2DOF control structure in which resonant regulators have been added.

The 2DOF controllers allow a fast tracking of the reference current component at the fundamental frequency of the grid. Moreover, it enables the damping of the LCL filter without the use of additional measurements, passive components or observers. On the other hand, the resonant regulators allow the tracking of the current harmonics.

A demonstration of how this control scheme can be used in an APF has been made through a HIL emulation of a typical application of such systems. A low interaction between the controllers has been achieved, with a total time response below a single period for the fundamental frequency component and three periods for its current harmonics.
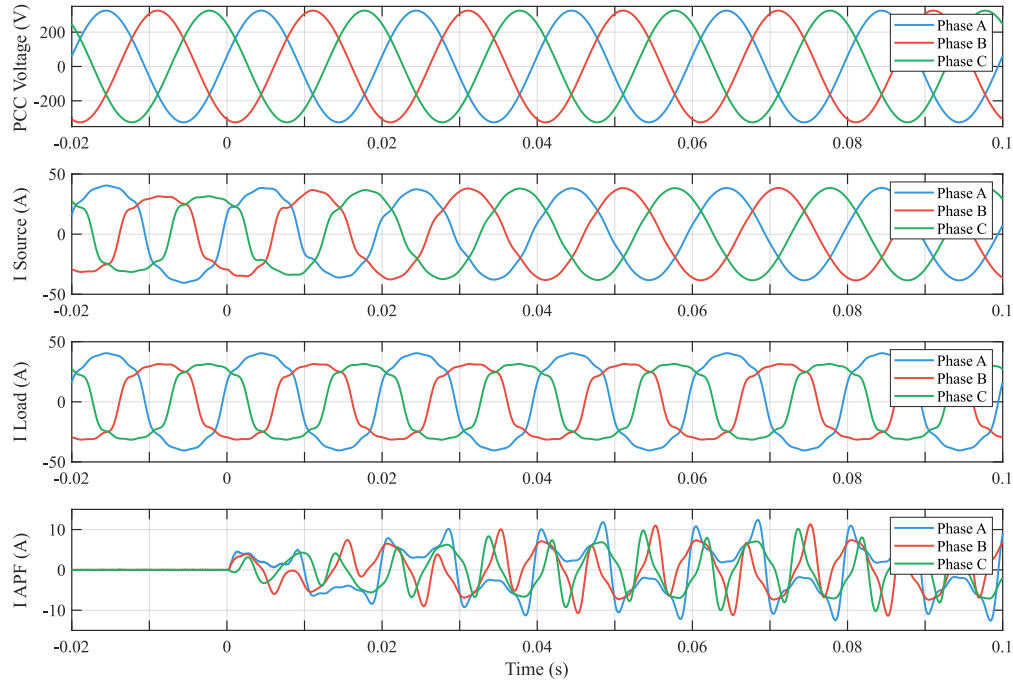
Fig. 9. Voltage at the PCC and currents in the source, loads and APF obtained during the transient response of the proposed control scheme.
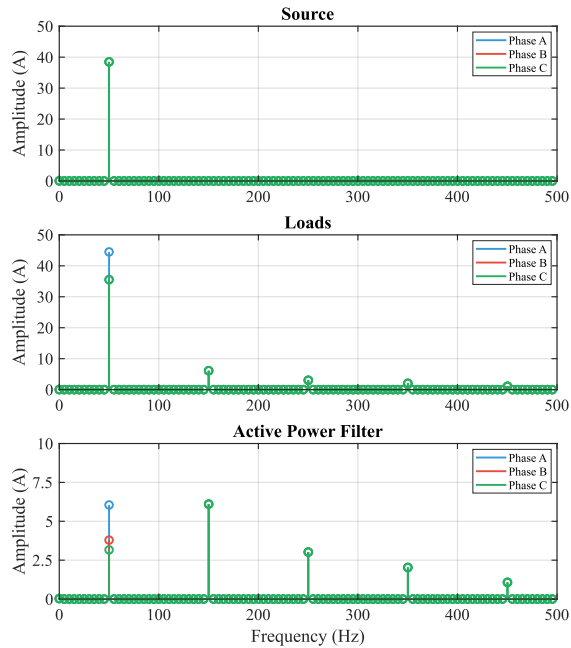
Fig. 10. FFT of the currents at the source, load and APF once the system has reached the steady state.

REFERENCES

[1] Q.-N. Trinh and H.-H. Lee, "An advanced current control strategy for three-phase shunt active power filters," *IEEE Transactions on Industrial Electronics*, vol. 60, no. 12, pp. 5400–5410, dec 2013.

[2] M. Liserre, R. Teodorescu, and F. Blaabjerg, "Multiple harmonics control for three-phase grid converter systems with the use of pi-res current controller in a rotating frame," *IEEE Transactions on Power Electronics*, vol. 21, no. 3, pp. 836–841, 2006.

[3] S. Bosch, J. Staiger, and H. Steinhart, "Predictive current control for an active power filter with LCL-filter," *IEEE Transactions on Industrial Electronics*, vol. 65, no. 6, pp. 4943–4952, jun 2018.

[4] G. Pandove and M. Singh, "Robust repetitive control design for a three-phase four wire shunt active power filter," *IEEE Transactions on Industrial Informatics*, vol. 15, no. 5, pp. 2810–2818, 2019.

[5] B. Singh, K. Al-Haddad, and A. Chandra, "A review of active filters for power quality improvement," *IEEE Transactions on Industrial Electronics*, vol. 46, no. 5, pp. 960–971, Oct 1999.

[6] P. Rodriguez, R. Pindado, and J. Bergas, "Alternative topology for three-phase four-wire pwm converters applied to a shunt active power filter," in *IEEE 2002 28th Annual Conference of the Industrial Electronics Society. IECON 02*, vol. 4, Nov 2002, pp. 2939–2944 vol.4.

[7] K. Haddad, T. Thomas, G. Joos, and A. Jaafari, "Dynamic performance of three phase four wire active filters," in *Proceedings of APEC 97 - Applied Power Electronics Conference*, vol. 1, Feb 1997, pp. 206–212 vol.1.

[8] F. J. Lopez-Alcolea, E. J. Molina-Martinez, J. Vazquez, A. P. Torres, P. Roncero-Sanchez, A. Moreno-Munoz, J. Garrido-Zafra, and F. Garcia-Torres, "Detection and compensation of current harmonics in a microgrid using an active power filter supported by an IoT sensor network," in *2021 IEEE International Conference on Environment and Electrical Engineering and 2021 IEEE Industrial and Commercial Power Systems Europe (EEEIC / I&CPS Europe)*. IEEE, sep 2021.

[9] A. Parreno Torres, F. J. Lopez-Alcolea, P. Roncero-Sanchez, J. Vazquez, E. J. Molina-Martinez, and F. Garcia-Torres, "Current control of a grid-connected single-phase voltage-source inverter with LCL filter," in *2020 22nd European Conference on Power Electronics and Applications (EPE'20 ECCE Europe)*. IEEE, sep 2020.

[10] A. Parreno Torres, P. Roncero-Sanchez, J. Vazquez, F. J. Lopez-Alcolea, and E. J. Molina-Martinez, "A discrete-time control method for fast transient voltage-sag compensation in DVR," *IEEE Access*, vol. 7, pp. 170 564–170 577, 2019.

[11] A. García-Cerrada, P. Roncero-Sánchez, P. García-González, and V. Feliú-Batlle, "Detailed analysis of closed-loop control of output-voltage harmonics in voltage-source inverters," *IEE Proceedings - Electric Power Applications*, vol. 151, pp. 734–743(9), November 2004.

[12] A. Reznik, M. G. Simões, A. Al-Durra, and S. M. Muyeen, "LCL filter design and performance analysis for grid-interconnected systems," *IEEE Transactions on Industry Applications*, vol. 50, no. 2, pp. 1225–1232, March 2014.